

Structural, morphology and optical properties of $\text{Zn}_{(1-x)}\text{Cd}_x\text{O}$ solid solution grown on c-plane sapphire substrate

A. Fouzri^{1,a}, M. A. Boukadhaba², M. Oumezzine², A. Bchetnia³ and V. Sallet⁴

¹Laboratoire Physico-chimie des Matériaux, Unité de Service Commun de Recherche « High resolution X-ray diffractometer », Département de Physique, Université de Monastir, Faculté des Sciences de Monastir, Avenue de l'Environnement, 5019 Monastir, Tunisia.

²Laboratoire Physico-chimie des Matériaux, Département de Physique, Université de Monastir, Faculté des Sciences de Monastir, Avenue de l'Environnement, 5019 Monastir, Tunisia.

³Unité de recherche hétéroépitaxie et ses applications, Département de Physique, Université de Monastir, Faculté des Sciences de Monastir, Avenue de l'Environnement, 5019 Monastir, Tunisia.

⁴Groupe d'Etude de la Matière Condensée, Centre National de la Recherche Scientifique/Université de Versailles Saint Quentin en Yvelines, UMR 8635, Paris France.

Abstract. $\text{Zn}_{(1-x)}\text{Cd}_x\text{O}$ solid solutions with a composition ranging from pure ZnO up to $x=0.046$ have been grown on c-plane sapphire substrates by using metal organic chemical vapor deposition (MO-CVD). The lattice deformation, morphology and optical properties of these films were examined in detail using high resolution X-ray diffraction, atomic force microscopy (AFM) and photoluminescence (PL) as Cd incorporation. Our study reveals significant microstructure modification of $\text{Zn}_{(1-x)}\text{Cd}_x\text{O}$ from $x \geq 0.7\%$ but single phase of wurtzite structure is maintained for all films. The PL spectra and the band gap of the $\text{Zn}_{(1-x)}\text{Cd}_x\text{O}$ film show red shift to visible light range which is interpreted in terms of band gap modulation due to Cd incorporation. Increase of Cd content leads to the emission broadening with growing lower energy peak (at 10K) and degraded crystallinity.

1 Introduction

ZnO is a II-VI wide band gap (3.3 eV) semiconductor material and has an ability to modulate the band to lower level by alloying with CdO [1]. ZnO has a wurtzite structure ($a=3.25 \text{ \AA}$, $c=5.21 \text{ \AA}$). CdO has rock salt (RS) structure ($a=4.70 \text{ \AA}$). The choice of CdO is based on the fact that ionic radius of Cd^{2+} (0.95 \AA) is close to that of Zn^{2+} (0.74 \AA), that is, wurtzite phase alloy can be expected in spite of RS structure of CdO. The thermodynamic solubility limit of CdO in ZnO has been reported to be less 2 mol% according to the phase diagram of the ZnO-CdO- P_2O_5 ternary system [2]. Although good results have been reported for homoepitaxially grown ZnO film [3], the high cost and limited availability of high-quality bulk ZnO substrates preclude their use in mass production environments. On the contrary, sapphire has been chosen as a substrate material due to its relatively low cost, availability in large area wafers. Many studies on the growth of ZnO films have used c-plane sapphire as substrate [4-11]. However, the heteroepitaxy of ZnO on sapphire presents several problems due to differences in their chemical nature, structure and lattices parameters [12]. Furthermore, it is known that the properties of thin solid film are closely related to its microstructure, morphology and surface roughness.

In our work, we are using optical transmission measurements to estimated cadmium incorporation, high-resolution X-ray diffraction (HRXRD), atomic force microscopy (AFM) and photoluminescence to analyses the structural, morphology and optical properties of $\text{Zn}_{(1-x)}\text{Cd}_x\text{O}$ solid solutions grown, by metal organic chemical vapor deposition (MO-CVD), on c-plane sapphire substrate as Cd incorporation.

^a e-mail : Fouzri.Afif@gmail.com

Article available at <http://www.epj-conferences.org> or <http://dx.doi.org/10.1051/epjconf/20122900019>

2 Experiments

The layer is grown in horizontal MO-CVD reactor at atmospheric pressure under N_2 carrier gas. Diethyl-Zinc (DEZn), Dimethyl-Cadmium (DMCd) and tertiary butanol (ter-butanol) are used as Zn, Cd and oxygen precursors, respectively at a growth temperature of $380^\circ C$. The growth conditions are described elsewhere [13]. With similar growth parameters, thin films of $Zn_{(1-x)}Cd_xO$ are directly deposited on c-plane sapphire substrates from Crystec. In order to obtain different compositions of cadmium, the molar flow rate of DMZn was maintained constant while that of DECD was gradually increased from 1 to 10 cc. The growth parameters of a series of five samples with different compositions are listed in table 1.

Table 1. MO-CVD growth parameters, energy band gap (E_g) and cadmium content at % of $Zn_{(1-x)}Cd_xO$ solid solutions deposited on c-plane sapphire substrate.

Sample	DEZn Pressure (Pa)	DMCd Pressure (Pa)	E_g (eV)	x (%)
M1	13	0	3.26	0
M2	26	1.5	3.24	0.5
M3	26	2.5	3.23	0.7
M4	26	5	3.14	3
M5	26	10	3.07	4.6

Thickness of ZnCdO film deposited on c-plane sapphire substrate for the different flux ratios used (0, 1, 2.5, 5 and 10 cc) are respectively about $1 \mu m$, $0.6 \mu m$, $2.2 \mu m$, $1.6 \mu m$ and $1.4 \mu m$ which are measured from cross-section SEM images (Figure 1). They clearly show the non-uniformity of layers thickness.

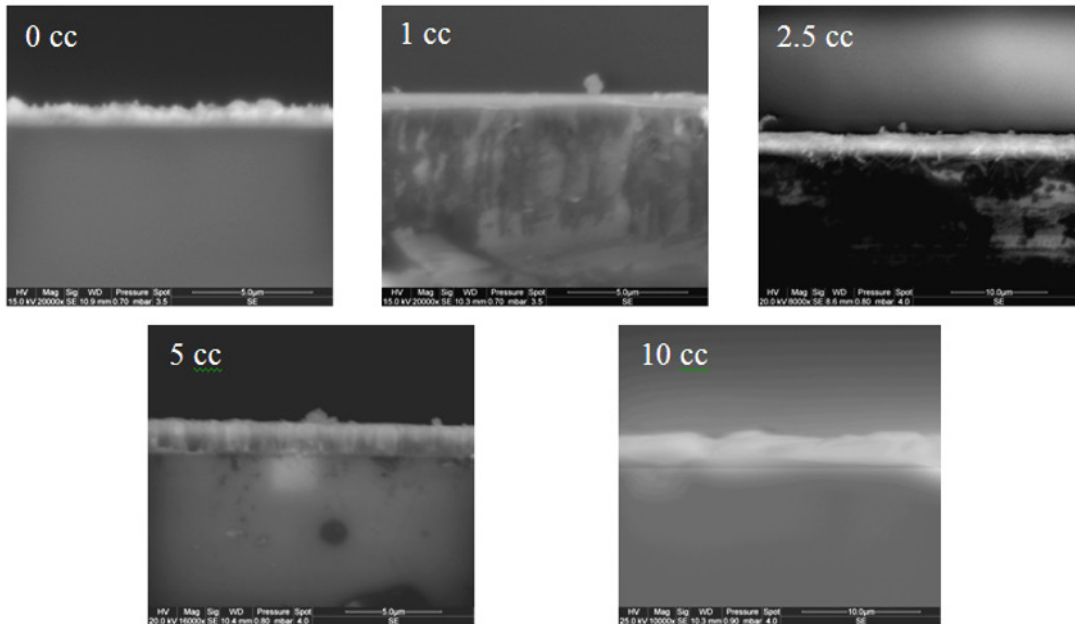


Fig. 1. Cross section SEM images of $Zn_{(1-x)}Cd_xO$ deposited on c-plane sapphire substrates for the different flux ratios used.

These samples are characterized by optical transmission measurements at 300K, in the range 310 – 690 nm using a DR/4000U spectrophotometer which can return either the absorption coefficient in arbitrary units or the transmittance in percentage. Figure 2 shows the square (αE) for the $Zn_{(1-x)}Cd_xO$ solid solution deposited on c-plane sapphire substrate as a function of the photon energy E . The absorption band-edge energy of these samples is estimated by extrapolating linear part of $(\alpha E)^2$ to zero. As seen here, the $Zn_{(1-x)}Cd_xO$ films shows shrinkage in energy gap, which provides supportive evidence that Cd incorporates in ZnO. The cadmium contents (table 1) in these layers deposited on c-plane sapphire substrate are determined from energy band gap (E_g) equation established by T. Makino et al. [14], where we have used $E_g(x=0)$ deduced from reference sample M1. The highest Cd content reached is 4.6% which is over twice larger than the thermodynamic solubility limit.

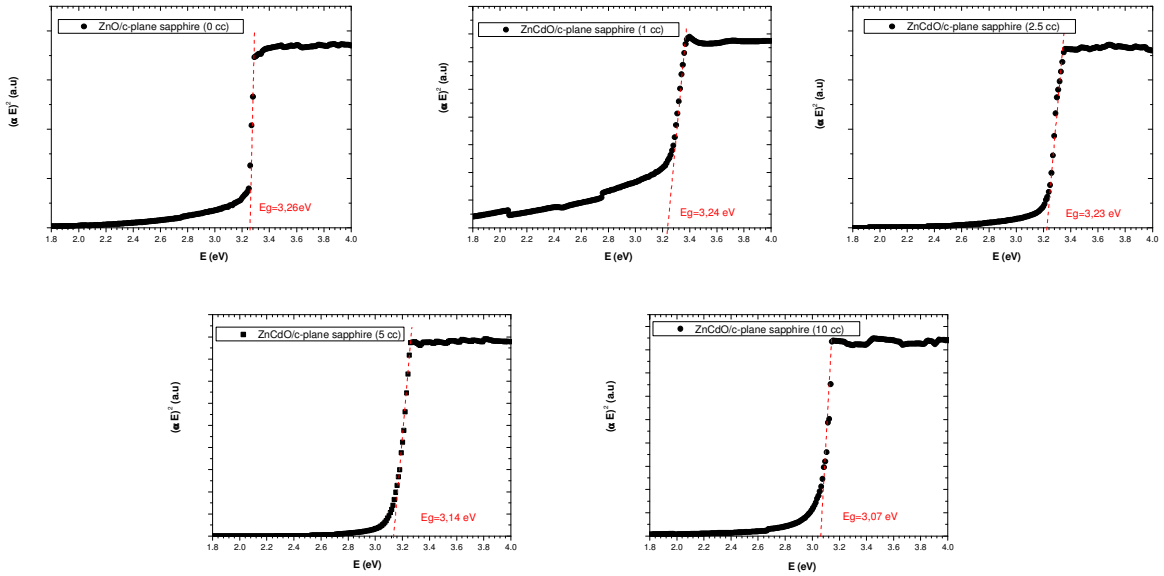


Fig. 2. Plots of the square (αE) as a function of photon energy (E) for the $Zn_{(1-x)}Cd_xO$ solid solution deposited on c-plane sapphire substrate for the different flux ratios used.

High-resolution X-ray diffraction (HRXRD) experiments were performed with D8 discover Bruker AXS diffractometer using $CuK_{\alpha 1}$ radiation at 1.5406 Å. The 2θ - θ scan revealed that all the films had c-axis orientation and wurtzite phase. No indication of any rocksalt phase related to segregate CdO within the layers could be detected. For illustration, XRD measurements of ZnO and $Zn_{(1-x)}Cd_xO$ ($x=4.6\%$) grown on c-plane sapphire are represented in Figure 3. In addition to the ZnO (0002) reflexion and its harmonic, we observe (0006) and (00012) reflexion corresponding to c-plane sapphire substrate.

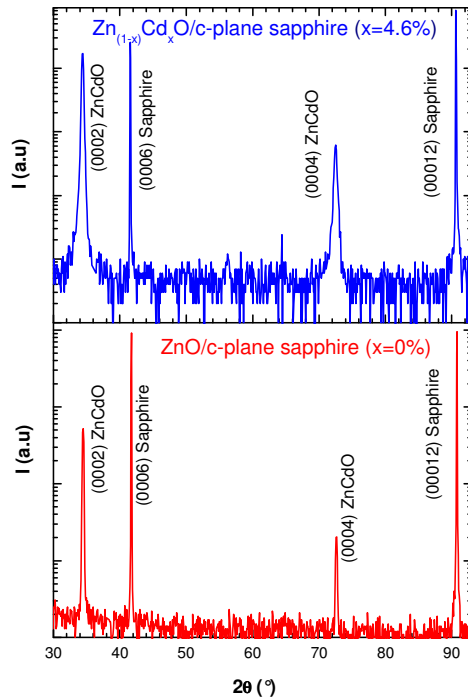


Fig. 3. 2θ - θ scan pattern of ZnO and $Zn_{(1-x)}Cd_xO$ ($x=4.6\%$) grown on c-plane sapphire.

The mosaicity of the film can be characterized by measuring the corresponding ω -rocking curve of the ZnO (0002) diffraction peak. The full widths at half maximum (FWHMs) of the layers peak are higher than 2° indicating a bad crystalline quality of layers. We have used high resolution X-ray diffraction on several symmetric (00.l) and several pairs of asymmetric (h0.l) reflections enabling us to precisely measure layer lattice parameters. The lattice parameters of $Zn_{(1-x)}Cd_xO$ deposited on c-plane sapphire are

determined and summarized in table 2. No layer lattice parameter was determined for sample M2 ($x=0.5\%$) because of the small film thickness.

Table 2. Lattice parameters, c/a ratio and cell volume of $Zn_{(1-x)}Cd_xO$ solid solutions deposited on c -plane sapphire as function of cadmium content x .

Sample	Cd content (%)	a (Å)	c (Å)	c/a	Cell volume (Å ³)
M1	0	3.251	5.206	1.601	47.65
M2	0.5	-	-	-	-
M3	0.7	3.251	5.206	1.601	47.65
M4	3	3.253	5.208	1.601	47.71
M5	4.6	3.261	5.215	1.599	48.02

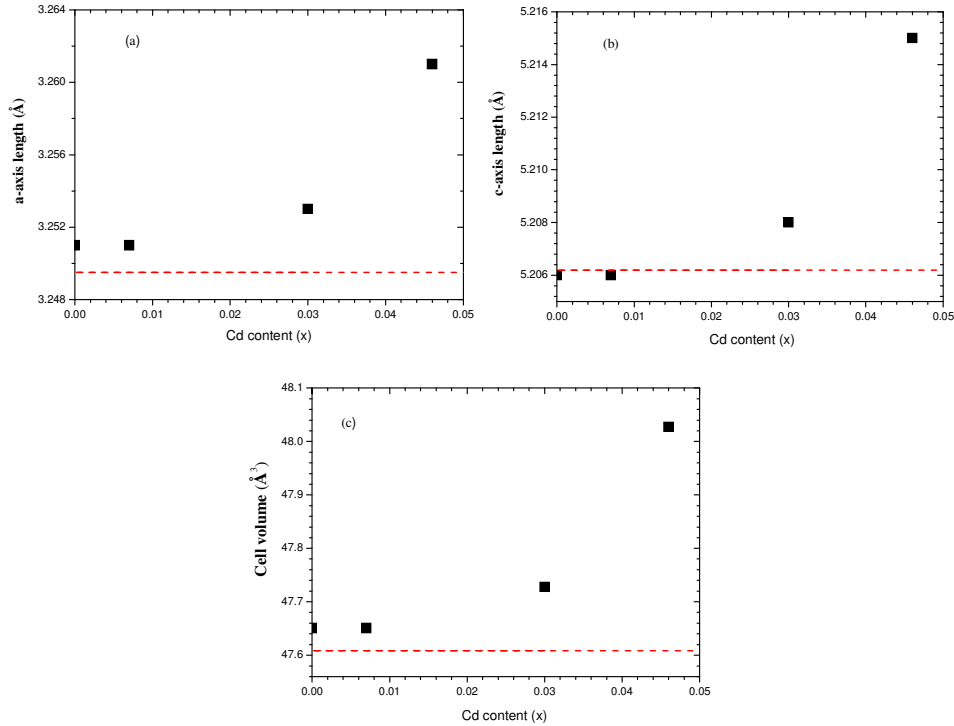


Fig. 4. Cadmium content x dependence of (a) a -axis lattice length, (b) c -axis lattice length and (c) the cell volume. In all cases the dashed line represents the corresponding parameters of bulk ZnO [15].

Compared to the bulk crystal values ($a=3.2495$ Å and $c=5.2062$ Å) [15], there is a slight lattice deformation, assuming that the layer is partially relaxed. The a -, c -axis lengths determined by HRXRD and the cell volume are plotted as functions of Cd content in Figure 4 (a), (b) and (c) respectively. The experimental errors of lattice parameter for all layers are estimated to be 0.003 Å. There is a significant change, compared to ZnO layer grown on c -plane sapphire, of a , c layers lattice parameters and the unit cell volume for cadmium content higher than 0.7% . Since for Cd content below 0.7% the $Zn_{(1-x)}Cd_xO$ parameter layer mimics that of the ZnO layer. By comparing a and c lattice parameters with those calculated by the evolution equation established by Makino et al. [14], we note that the in - of - plane lattice parameters are similar, however those out -of - plane are different.

At higher cadmium content, the cell volume varied 0.8% for the layer grown on sapphire substrate from that of bulk ZnO. For the film deposited on ZnO, this variation is half of the predicted value (1.6%) obtained by assuming that this difference is caused by the difference in the cation radii of Cd^{2+} (0.95 Å) and Zn^{2+} (0.74 Å). The ratio (c/a) is between 1.601 and 1.599 for all layers deposited on sapphire which differed very little from those of bulk ZnO ($c/a=1.602$). The in-plane (ϵ_{xx}) and out-plane (ϵ_{zz}) epitaxial strain is calculated and plotted in Figure 5 as function of cadmium content. We have used the lattice parameters of ZnO completely relaxed (bulk) [15]. We can note that the deformation in the growth plan is nearly two times more important than that out of the plane for $x>0.7\%$.

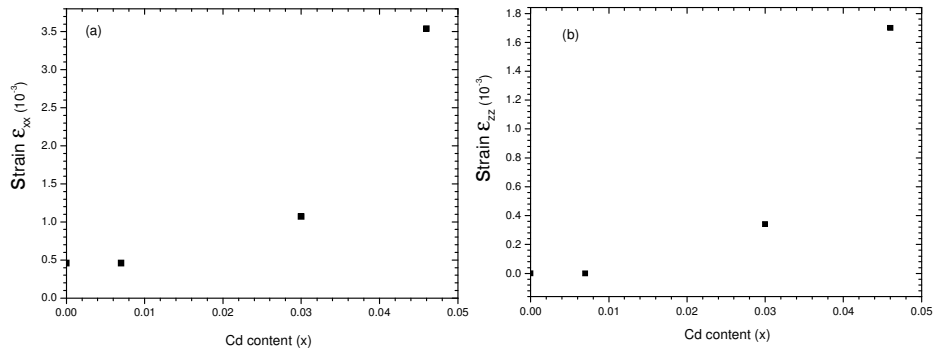
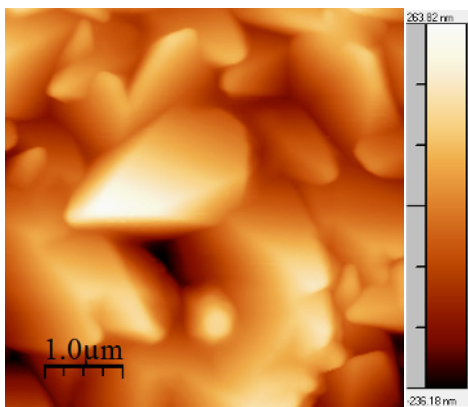
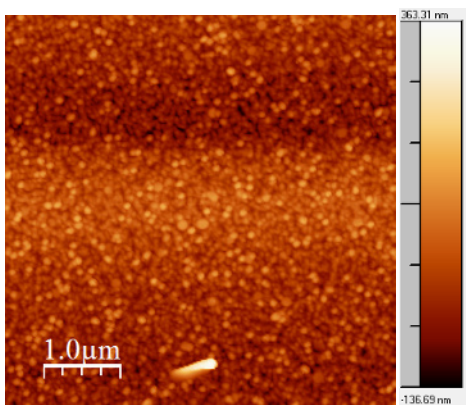
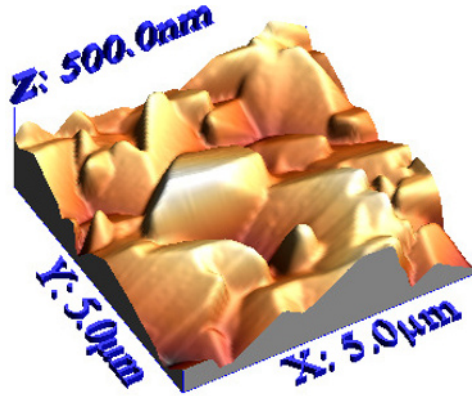


Fig. 5. Epitaxial strain ϵ_{xx} (a) and ϵ_{zz} (b) of $\text{Zn}_{(1-x)}\text{Cd}_x\text{O}$ /c-plane sapphire as a function of cadmium content x .

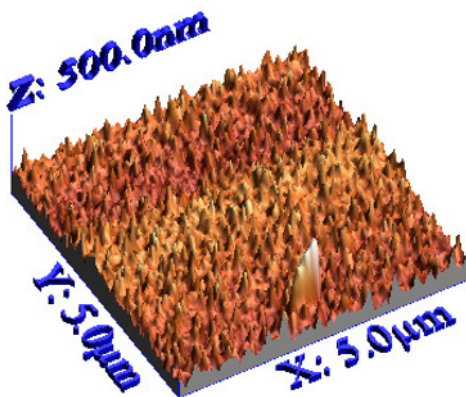
The surface morphology of our film was observed by atomic force microscopy (AFM). All the AFM images were recorded with a Nanoscope III a microscope from digital instruments Inc. in the tapping mode (25°C, in air). The film morphology of $\text{Zn}_{(1-x)}\text{Cd}_x\text{O}$ grown on c-plane sapphire (scan area $5\mu\text{m} \times 5\mu\text{m}$) are shown in Figure 6. The AFM images are shown in three and two dimensions to see the difference in the morphology of layers as function of cadmium. The surface roughness of different samples was calculated from AFM images using the software “NanoRule” and the values obtained are presented in table 3.

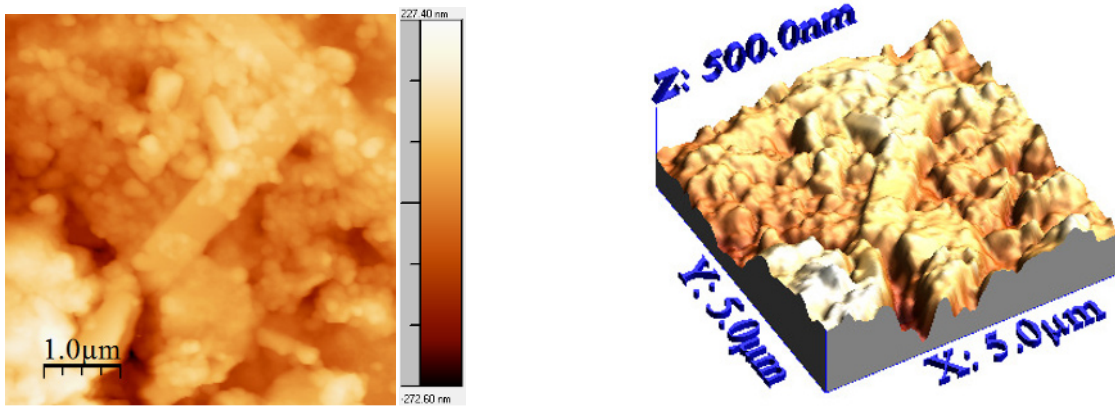


ZnO /c-plane sapphire ($x=0\%$)

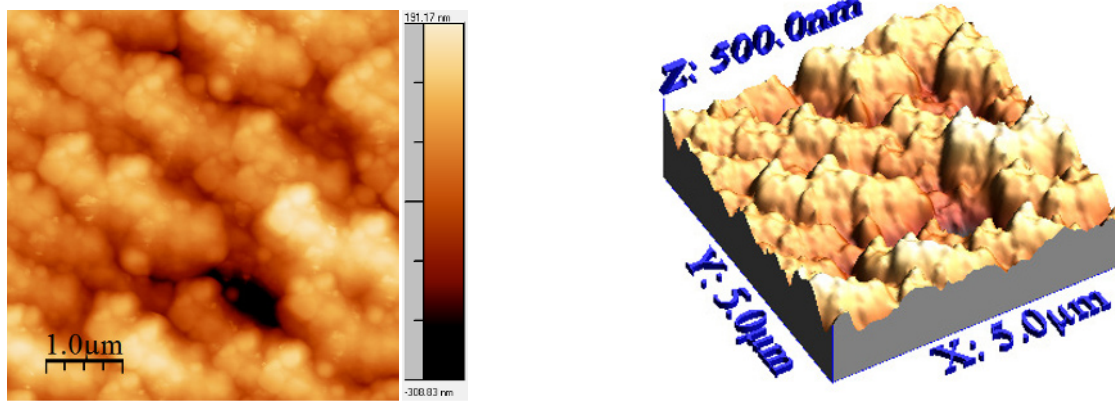


$\text{Zn}_{(1-x)}\text{Cd}_x\text{O}$ /c-plane sapphire ($x=0.5\%$)

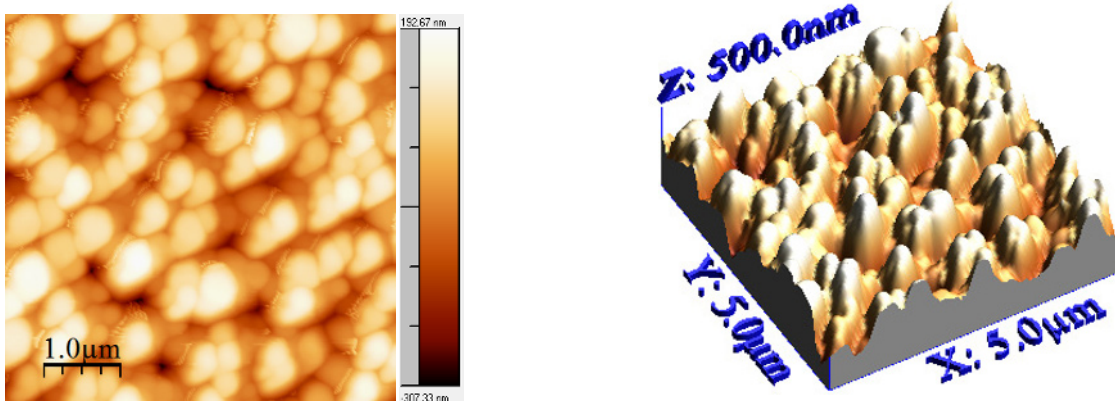




$Zn_{(1-x)}Cd_xO/c\text{-plane sapphire}$ ($x=0.7\%$)



$Zn_{(1-x)}Cd_xO/c\text{-plane sapphire}$ ($x=3\%$)



$Zn_{(1-x)}Cd_xO/c\text{-plane sapphire}$ ($x=4.6\%$)

Fig. 6. 3D (right) and 2D (left) AFM images of $Zn_{(1-x)}Cd_xO$ deposited on c-plane sapphire as function of Cd content.

Upon inspection of the images, ZnO deposited on c-plane sapphire the surface morphology consists of big and faceted grains with rms surface roughness of about 85nm. For solid solutions, the morphology surfaces appear rather rounded grain with a lower surface roughness. However, it is very difficult to correlate the change in surface roughness to that of cadmium content, especially since the film thicknesses are different. The change in grain shape is probably caused by the presence and relative orientations of the different areas of the charges resulted from the atomic arrangement but are disturbed by the incorporation of cadmium and the nature of the surface [16, 17].

Table 3. Roughness surface of $Zn_{(1-x)}Cd_xO$ layers grown on c-plane sapphire for the different cadmium content.

Sample	Cd content (%)	Roughness surface (nm)
M1	0	85
M2	0.5	15
M3	0.7	45
M4	3	30
M5	4.6	60

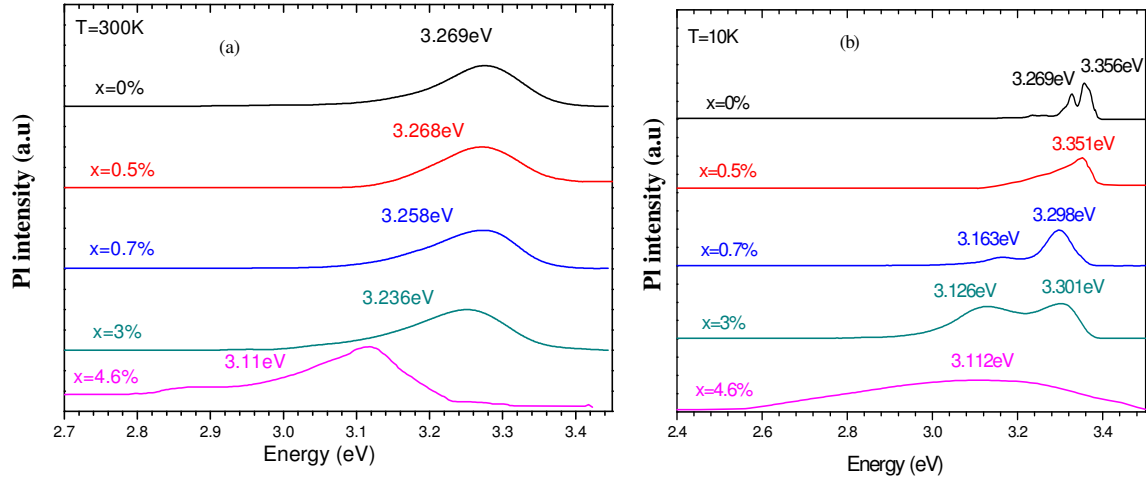


Fig. 7. Photoluminescence of different Zn_(1-x)Cd_xO solid solutions grown on c-plane sapphire substrate (a) at 300K and (b) at 10K.

Photoluminescence (PL) measurements were made for these different layers at room temperature using the 325 nm line of He-Cd laser. PL spectra at 10K and 300K of Zn_(1-x)Cd_xO solid solutions grown on c-plane sapphire as function of cadmium content are shown in Figure 7 (a) and (b). The observed PL peak at room temperature of solid solutions shifts to lower energies corresponding to the excitonic emission band when the cadmium content x increases. The full width at half maximum (FWHM) is about 130 meV for $x \leq 3\%$ and about 150 meV for $x = 4.6\%$. The PL spectra at low temperature show the disappearance of the typical fine structure of ZnO [18-24] and the appearance of the shoulder at low energy which becomes more intense and wide as x increases. This is presumably due to larger compositional fluctuation and poorer crystallinity for larger x films. In fact, low temperature PL spectroscopy is a suitable method to detect inhomogeneous potential fluctuation because the photo-excited carriers cannot travel long distance resulting in radiative recombination after relaxation into local potential minima. This same findings were reported by M. Kawasaki [25] with Zn_(1-x)Cd_xO films grown on sapphire (0001) substrates by pulsed laser deposition.

3 Conclusion

Zn_(1-x)Cd_xO solid solutions have been grown on c-plane sapphire substrate by metal organic chemical vapor deposition with the DMCD molar ratio range 0 to 10cc. The cadmium mole fraction was determined from energy band gap equation established by T. Makino [14]. Cd content has been seen to increase monotonically with the DMCD molar ratio until about $x = 4.6\%$ which is significantly larger than thermodynamic solubility limit (2%). The XRD study revealed that all layers exhibit a wurtzite phase and had a c-axis orientation. ω rocking curve measurement shows a poorer crystalline quality of layer. The microstructure of Zn_(1-x)Cd_xO layer grown on c-plane sapphire substrate compared to the reference sample M1, shows a significant modification from $x \geq 0.7\%$. The Photoluminescence spectra show a gradual red shift indicating the narrowing of the band gap due to cadmium incorporation. Even though, it is difficult to obtain high-crystalline quality Zn_(1-x)Cd_xO films due to necessary low temperature growth, we can conclude that this material is potential candidate for an active layer in blue LED based on ZnO.

Acknowledgements

The authors thank Dr.N.Sakly (LPCI, Faculty of Science of Monastir, Tunisia) for AFM characterization.

References

1. A. Nakamura, J. Ishihara, S. Shigemori, K. Yamamoto, T. Aoki, H. Gotoh, J. Temmyo, Jpn. J. Appl. Phys. Part 2 **44**, L4 (2005)
2. J. J. Brown, F. A. Hummel, J. Electron. Soc. **111**, 1056 (1964)
3. K. Agata, K. Maejima, Sz. Fujita, J. Cryst. Growth. **248**, 25 (2003)
4. P. Fons, K. Iwata, S. Niki, A. Yamada, K. Matsubara, J. Cryst. Growth. **201/202**, 627 (1999)
5. R. D. Vispute, V. Talyansky, Z. Trajanovic, S. Choopun, R. Downes, R. P. Sharma, T. Venkatesan, Appl. Phys. Lett. **70** (20), 2735 (1997)
6. E. S. Shim, H.S. Kang, J.S. Kang, J.H. Kim, S.Y. Lee, Appl. Surf. Sci. **186**, 474 (2002)
7. V. Sallet, C. Thiandoume, J.F. Rommeluere, A. Lusson, A. Riviere, J.P. Riviere, O. Gorochoy, R. Triboulet, V. Muñoz-Sanjosé, Mater. Lett. **53**, 126 (2002)
8. T. Gruber, C. Kirchner, K. Thonke, R. Sauer, A. Waag, Phys. Stat. Sol. A **192**, 166 (2002)
9. S. H. Lim, D. Shindo, H.B. Kang, K. Nakamura, J. Cryst. Growth **225**, 208 (2001)
10. A. Ohtomo, M. Kawasaki, Y. Sakurai, Y. Yoshida, H. Koinuma, P. Yu, Z.K. Tang, G.K.L. Wong, Y. Segawa, Mater. Sci. Eng. B **54**, 24 (1998)
11. F. Vigué, P. Vennéguès, S. Vézian, M. Laügt, J.P. Faurie, Appl. Phys. Lett. **79**, 194 (2001)
12. D. F. Croxal, R. C. C. Ward, C. A. Wallace, R. C. Kell, J. Cryst Growth **22**, 117 (1974)
13. J. Zúñiga-Pérez, V. Muñoz-Sanjosé, M. Loreng, G. Benndorf, S. Heitsch, D. Spemann, M. Grundmann, J. Appl. Phys. **99**, 023514 (2006)
14. T. Makino, Y. Segawa, M. Kawasaki, A. Ohtomo, R. Shiroki, K. Tamura, T., Yasuda, H. Koinuma, Appl. Phys. Lett. **78**, 1237 (2001)
15. F. Vigué, P. Vennéguès, C. Deparis, S. Vézian, M. Laügt, J. P. Faurié: J. Appl. Phys. **90**, 5115 (2001)
16. J. Zúñiga-Pérez, V. Muñoz-Sanjosé, E. Palacio-Lidon, J. Colchero, Appl. Phys. Lett. **88**, 261912 (2006)
17. J. Zúñiga-Pérez, E. Palacio-Lidon, V. Muñoz-Sanjosé, J. Colchero : Phys. Rev. Lett. **95**, 226105 (2005)
18. D. C. Reynolds, C. W. Litton, T. C. Collins, Phys. Rev. **140**, A1726 (1965).
19. Ü. Özgür, Ya. I. Alivov, C. Liu, A. Teke, M. A. Reshchikov, S. Doğan, V. Avrutin, S.-J. Cho, H. Morkoç, Appl. Phys. rev **98**, 041301 (2005)
20. D. C. Reynolds, D. C. Look, B. Jogai, C. W. Litton, G. Cantwell, W. C. Harsch, Phys. Rev. B **60**, 2340 (1999)
21. B. K. Meyer, H. Alves, D. M. Hofmann, W. Kriegseis, D. Forster, F. Bertram, J. Christen, A. Hoffmann, M. Strassburg, M. Dworzak, U. Habocek, A. V. Rodina, Phys. Stat. Sol. (b) **241**, 231 (2004)
22. C. Gonzales, D. Block, R. T. Cox, A. Hervé, J. Cryst. Growth **59**, 357 (1982)
23. A. Teke, Ü. Özgür, S. DOgan, X. Gu, H. Morkoç, B. Nemeth, J. Nause, H. O. Everitt, Phys. Rev. B **70**, 195207 (2004)
24. B. K. Meyer, J. Sann, D. M. Hofmann, C. Neumann, A. Zeuner, Semicond. Sci. Technol. **20**, S62 (2005)
25. M. Kawasaki, A. Ohtomo, R. Shiroki, I. Ohkubo, H. Kimura, G. Isoya, T. Yasuda, Y. Segawa, and H. Koinuma, *Extended Abstracts of International Conference on Solid State Devices and Materials, Hiroshima, Japan*, 356 (1998).